TOPIC HIGHLIGHT

Jose Manuel Ramia, MD, PhD, FACS, *Series Editor*

Radiology of pancreatic neoplasms: An update

Luis Gijón de la Santa, José Antonio Pérez Retortillo, Ainhoa Camarero Miguel, Lea Marie Klein

Luis Gijón de la Santa, José Antonio Pérez Retortillo, Ainhoa Camarero Miguel, Lea Marie Klein, Department of Radiology, Guadalajara University Hospital, University of Alcalá, 19002 Guadalajara, Spain
Author contributions: Gijón de la Santa L designed research; Klein LM is a native speaker of English and revised the manuscript; Gijón de la Santa L, Pérez Retortillo JA were responsible for literature search and picture selection; Camarero Miguel A, Klein LM contributed to the literature review; all authors have contributed to the performed research and wrote the paper.
Correspondence to: Luis Gijón de la Santa, MD, Department of Radiology, Guadalajara University Hospital, University of Alcalá, Donantes de Sangre st, 19002 Guadalajara, Spain. lgijon@sescam.jccm.es
Telephone: +34-949-209200 Fax: +34-949-209218
Received: August 8, 2013 Revised: October 8, 2013
Accepted: December 12, 2013
Published online: September 15, 2014

Core tip: Diagnostic imaging is an important tool to evaluate pancreatic neoplasms. We describe and illustrate the imaging features and key findings of pancreatic malignancies and their mimics. The knowledge of radiologic findings is relevant to do an accurate diagnosis that allows a proper management and should be known not only for radiologists but by physicians that comprise multidisciplinary teams.

Abstract

Diagnostic imaging is an important tool to evaluate pancreatic neoplasms. We describe the imaging features of pancreatic malignancies and their benign mimics. Accurate detection and staging are essential for ensuring appropriate selection of patients who will benefit from surgery and for preventing unnecessary surgeries in patients with unresectable disease. Ultrasound, multidetector computed tomography with multiplanar reconstruction and magnetic resonance imaging can help to do a correct diagnosis. Radiologists should be aware of the wide variety of anatomic variants and pathologic conditions that may mimic pancreatic neoplasms. The knowledge of the most important characteristic key findings may facilitate the right diagnosis.

INTRODUCTION

Diagnostic imaging is an important tool to evaluate pancreatic neoplasms. Accurate detection and staging are essential for ensuring appropriate selection of patients who will benefit from surgery and for preventing unnecessary surgeries in patients with unresectable disease[1,2]. Ultrasound (US), multidetector computed tomography (MDCT) with multiplanar reconstruction and magnetic resonance imaging (MRI) can help to do a correct diagnosis[3,4].

A wide variety of anatomic variants and pathologic conditions exist that may mimic pancreatic neoplasms. Pancreas such as pancreas divisum or anular pancreas may cause enlargement of the pancreatic head and be mistaken for a tumoral mass. Non-distended adjacent bowel, gastric fundus, duodenal diverticula, duplications[2,5-7] accessory spleen or splenosis may also mimic a pancreatic mass[8]. Chronic pancreatitis may be indistinguishable from neoplasm on the basis of morphologic at MRI and MDCT[9] (Figure 1). Positron emission tomography (PET) with 2-[18F]-fluoro2-deoxy-d-glucose (FDG)/MRI fusion image significantly improved accu-

Table 1 Pancreatic tumors

Pancreatic tumors
Primary (95%)
Solid tumors
Pancreatic adenocarcinoma (85%-95%)
Pancreatic neuroendocrine tumor
Solid pseudopapillary tumor
Pancreatoblastoma
Pancreatic lymphoma
Cystic tumors
Serous cystadenoma
Mucinous cystic neoplasm
Intraductal papillary mucinous tumor
of the pancreas
Metastatic lesions (5%)

racy compared with that of PET/CT (in differentiating pancreatic cancer from benign lesions 96.6% *vs* 86.6%)[10].

Enlarged peripancreatic nodal chains and disease in surrounding structures can mimic pancreatic masses (gastric fundus neoplasm, small bowel tumors, renal or adrenal masses, *etc*.). The existence of fat planes between the nodes or tumoral masses and the pancreatic gland or displacement of the pancreas may be useful to distinguish these lesions from a pancreatic mass[6] (Figure 2). Choledochal cysts may simulate a cystic mass in the head of the pancreas[11].

True pancreatic masses can be classified in primary or metastatic lesions (Table 1).

PRIMARY PANCREATIC LESIONS

Primary pancreatic masses will be classified on the basis of its radiologic appearance in solid or cystic lesions.

SOLID LESIONS OF THE PANCREAS

Pancreatic adenocarcinoma

Pancreatic adenocarcinoma accounts for 85%-95% of all pancreatic malignancies and is the fourth leading cause of cancer-related deaths. Most patients are 60-80 years of age, and males are affected twice as often as females[3,4]. Of these tumors, 60%-70% are located in the pancreatic head, 10%-20% in the body, and 5%-10% in the tail. Diffuse glandular involvement occurs in 5% of cases[2,3]. Surgery is the only cure, with a postoperative 5-year survival rate of 20%[3,4]. Unresectable disease is seen at presentation in 75% of patients (Figure 3).

Dual-phase (arterial and portal) contrast material–enhanced MDCT is the established technique for evaluating pancreatic adenocarcinoma. Arterial phase imaging (performed 20-40 s after contrast agent injection) allows optimal visualization of the tumor and peripancreatic arteries (Figure 4). Portal phase imaging (performed 50-70 s after injection) is optimal for assessing the peripancreatic veins and detecting metastatic disease to the liver[3] (Figure 5). After intravenous contrast administration most tumors are hypoattenuating (Figure 6).

Figure 1 **Multidetector computed tomography image.** Multidetector computed tomography shows enlargement of the pancreatic head (arrow), with dilatation and beading of the pancreatic duct (arrowhead) and dilatation of the extra- and intrahepatic bile ducts. A focal calcification can also be visualized. These findings matched with the definite diagnosis of a chronic pancreatitis.

No pancreatic mass is visualized in 10% of cases, since the tumor may be isoattenuating. The presence and location of a mass may be inferred from secondary signs such as mass effect, an abnormal convex contour of the pancreas, ductal obstruction, and vascular invasion[2-4] (Figures 7 and 8). Tumors in the pancreatic head may cause dilatation of both common bile duct and the main pancreatic duct (MPD), known as the "double duct sign"; whereas tumors in the pancreatic body may cause upstream MPD dilatation (Figure 9A). A circumferential soft-tissue cuff around the peripancreatic vessels with loss of the perivascular fat plane denotes vascular invasion. A sensitivity of 84% and a specificity of 98% for invasion are reported if the tumor is contiguous with more than 50% of the vessel circumference[1] (Figure 9B). Other features suggesting vascular invasion include vessel deformity, thrombosis, and development of collateral vessels[12]. Cystic-necrotic degeneration, an uncommon feature of adenocarcinoma, is present in 8% of cases[13,14]. Metastases are most commonly found in the liver (Figure 5B) and peritoneum (Figure 9C)[2,3].

Adenocarcinoma has low signal intensity on T1 and T2 weighted MRI secondary to its scirrhous fibrotic nature (Figure 10). As at MDCT, the hypovascular tumor enhances less than the normal pancreas at MRI (Figure 11). MRI has better contrast resolution than MDCT and is superior in detecting small tumors and metastases[15]. Diffusion-weighted (DW) MRI allows the assessment of thermally induced random molecular motion in biologic tissues and generates representative apparent diffusion coefficient (ADC) values[16-18]. The use of DW MRI may allow earlier detection of pancreatic tumours, since these neoplasms have increased signal intensity on diffusion-weighted images and relatively low ADC values because of the restricted diffusion associated with fibrosis (Figure 12). In addition, DW MRI may be helpful in the detection of metastases in the liver and lymph nodes[16,17].

Endoscopic US has a recognized role in the detection and staging of small tumors. It can help detect masses as small as 0.2 cm. Endoscopic US can clarify equivocal find-
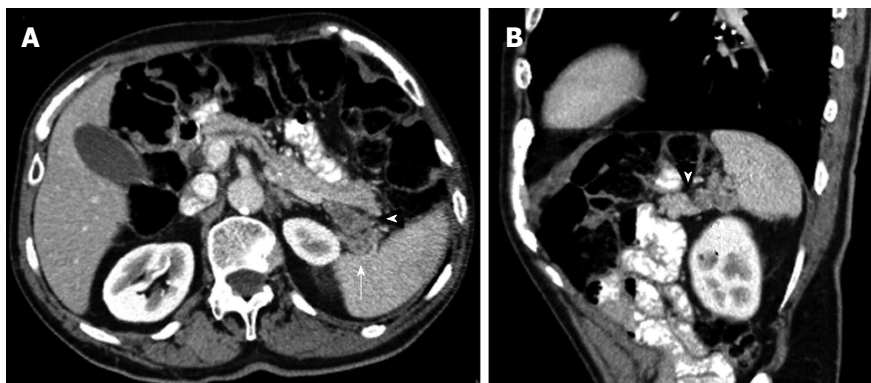
Figure 2 Axial contrast enhanced multidetector computed tomography image. A: Depicts a nodular peripancreatic mass localized between the pancreatic tail (arrowhead) and the splenic hilum (arrow), each well separated by fat planes; B: The sagittal reformatted contrast enhanced multidetector computed tomography image allows a better identification of the surrounding fat planes (arrow and arrowhead) enabling the exclusion of a pancreatic dependency. This mass actually turned out to be a tumoral implant of a gastric neoplasm.

Figure 3 Unresectablility of a pancreatic adenocarcinoma. Contrast enhanced multidetector computed tomography (MDCT) image (A) and coronal reformation image (B) shows dilatation of the distal pancreatic duct caused by a hypodense tumor (arrow) in the pancreatic body. On plain film (C) and coronal reformation image on MDCT (D) of the same patient multiple lung metastases of his pancreatic carcinoma are evident - a definite criteria for unresectability.

ings at MDCT or MRI and allows biopsy of suspect lesions. Adenocarcinoma appears as an ill-defined, heterogeneous hypoechoic mass at endoscopic US[3] (Figure 13).

PET is an emerging technique for characterizing tissue on the basis of functional rather than morphologic information. The principle of FDG PET is that malignant tissues have greater uptake and retention of FDG than does normal tissue due to enhanced glucose metabolism. Pancreatic adenocarcinoma generally shows intense focal FDG uptake. The biggest potential impact of FDG PET is in the detection of small metastases, an area in which MDCT and MRI generally underestimate lesions[3].

Pancreatic neuroendocrine tumor

Pancreatic neuroendocrine tumors (NETs) account for 1%-5% of all pancreatic tumors and typically manifest in patients aged 51-57 years. Most cases are sporadic, but association with syndromes such as multiple endocrine neoplasia type 1, von Hippel-Lindau syndrome, neurofibromatosis type 1, and tuberous sclerosis has been observed. Tumors tend to be multiple when associated with syndromes.

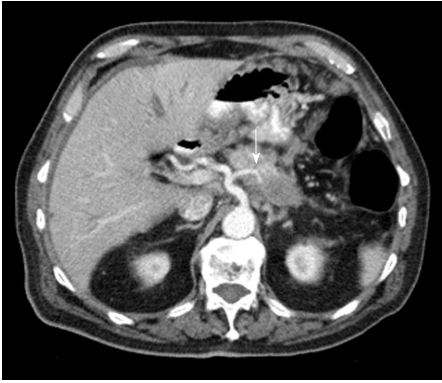NETs are classified into functioning and nonfunc-

Figure 4 Axial contrast enhanced multidetector computed tomography image. Arterial phase imaging allows optimal visualization of the pancreatic neoplasm and peripancreatic arteries: the shown hypodense mass compromises the splenic artery (arrow). Pancreatic adenocarcinoma was proven by biopsy.
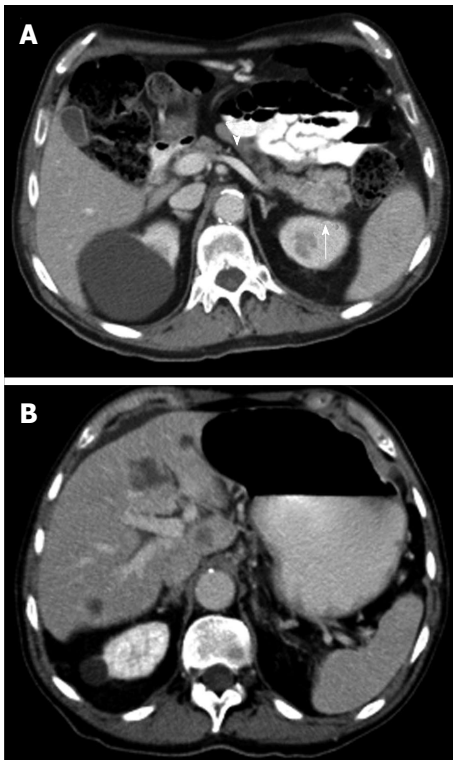

Figure 5 Contrast enhanced multidetector computed tomography image. A: In portal venous phase depicts a mass (arrow) in the pancreatic tail with permeability of the splenic vein (arrowhead); B: Focal round focal hypodensities with different sizes, localized in both hepatic lobules, represent metastatic spread to the liver. Pancreatic adenocarcinoma was proven by biopsy.

tioning tumors. Functioning tumors produce symptoms related to excessive hormone production. In general, functioning tumors manifest early in the course of disease. Nonfunctioning tumors manifest when they are large, due to mass effect. Risk of malignancy increases with tumor size (especially in tumors > 5 cm). Because of this fact 90% of nonfunctioning tumors are malignant at presentation[19].

Small tumors are generally solid and homogeneous, whereas larger tumors are heterogeneous and may show

Figure 6 Axial multidetector computed tomography image. Pancreatic tumor, localized in the pancreatic head (arrow), is hypodense in relation to the pancreatic parenchyma after contrast administration.

variable amounts of cystic-necrotic degeneration and calcification[3,19,20] (Figure 14).

NETs have a rich vascular supply and therefore enhance avidly during the arterial phase, enhancing more rapidly and intensely than the normal pancreas. That finding helps differentiate NETs from the more common adenocarcinoma which is hypovascular. Homogeneous enhancement is typical for small tumors (less than 2 cm), whereas larger lesions tend to show heterogeneous enhancement.

When NETs have a predominantly cystic component MDCT and MRI show a hypervascular enhancement in the nonnecrotic or nondegenerated portions of the tumor. Cystic areas are typically hyperintense at MRI on T2-weighted images (Figure 15).

Metastases to lymph nodes and solid organs such as the liver may have an enhancement pattern similar to that of the primary tumor (Figure 16). Cystic metastases to the liver may also be seen[3,19].

Solid pseudopapillary tumor

Solid pseudopapillary tumor (SPT) accounts for 1%-2% of all pancreatic tumors. It is most common in young females (mean age, 25 years)[21]. SPT has a low malignant potential with an excellent prognosis following complete resection.

SPT is typically a large (mean, 9 cm), slow-growing, well-encapsulated mass[21,22]. It most commonly occurs in the pancreatic tail. SPT has a tendency to displace rather than invade surrounding structures and rarely causes obstruction of the bile duct or pancreatic duct. MDCT usually demonstrates a well-encapsulated lesion with varying solid and cystic components owing to hemorrhagic degeneration[23]. Hemorrhage may progress to cystic changes within the lesions in approximately 20% of cases. Degenerated areas may mimic certain features of larger NETs. However, the peripheral portions of solid and papillary epithelial neoplasms do not demonstrate the hypervascularity typical of NETs[21]. SPT shows peripheral heterogeneous enhancement with central cystic spaces[24,25].
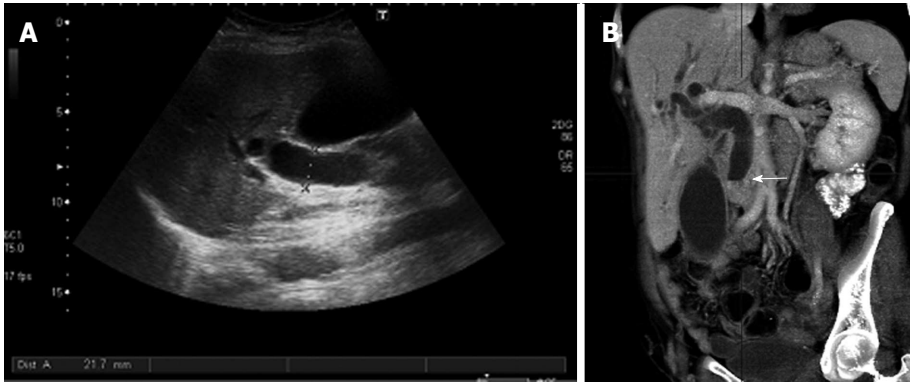
MRI typically demonstrates a well-defined lesion with

Figure 7 Indirect signs of pancreatic neoplasms. Transverse ultrasound image (A) shows a markedly dilated common bile duct, also seen on the coronal reformation image of multidetector computed tomography (B) where the dilated duct terminates abruptly at the level of the pancreatic head (arrow).

Figure 8 Endoscopic retrograde cholangiopancreatography. A short segment of narrowing causing stenosis of the common bile duct was recognized (arrow), without affection of the main pancreatic duct (arrowhead). Pancreatic adenocarcinoma was proven by biopsy.

heterogeneous signal intensity on T1- and T2-weighted images. Peripheral calcification is present in 30% of cases[21]. The pseudocapsule (composed of compressed pancreatic tissue and reactive fibrosis) has low attenuation at MDCT and low signal intensity at T_1- and T_2-weighted MRI.

Internal hemorrhagic and cystic degeneration is the hallmark of SPT due to the fragile vascular network of the tumor[3,26]. Although most SPTs exhibit benign behavior, malignant degeneration does occur. Metastases are uncommon, occurring in 7%-9% of cases, mostly to the liver, omentum, and peritoneum[27].

Pancreatoblastoma

Pancreatoblastoma accounts for 0.2% of all pancreatic tumors and is the most common pancreatic tumor in young children (mean 5 years)[3,28]. Pancreatoblastoma rarely occurs in adults; when it does, however, the tumor is generally more aggressive. The serum alpha-fetoprotein level is elevated in 25%-33% of cases[29].

Pancreatoblastoma is typically slow growing and generally manifests as an asymptomatic large mass (mean, 10 cm). Because of the large size of the mass at presentation, in 50% of cases it is not possible to identify the
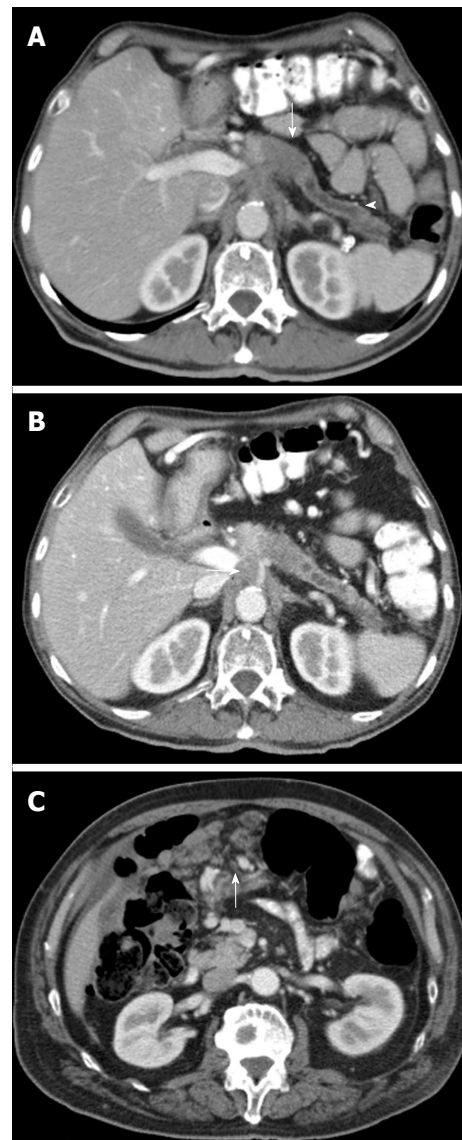

Figure 9 Axial contrast enhanced multidetector computed tomography image A: Focal hypodense mass in the body of the pancreas (arrow), with upstream dilatation of the main pancreatic duct (arrowhead). Pacreatic adenocarcinoma was histologically proven; B: Image depicts a circumferential soft tissue cuff around the celiac trunk according to vascular invasion (arrow); C: Image shows multiple peritoneal metastases in a patient with a pancreatic tumor (arrow).
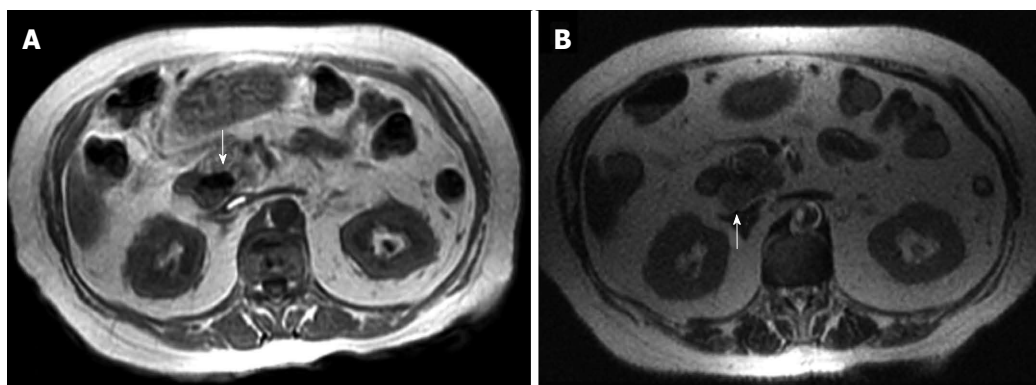
Figure 10 Adenocarcinoma has low signal intensity on T1 (A) and T2 (B) weighted magnetic resonance imaging (arrows).
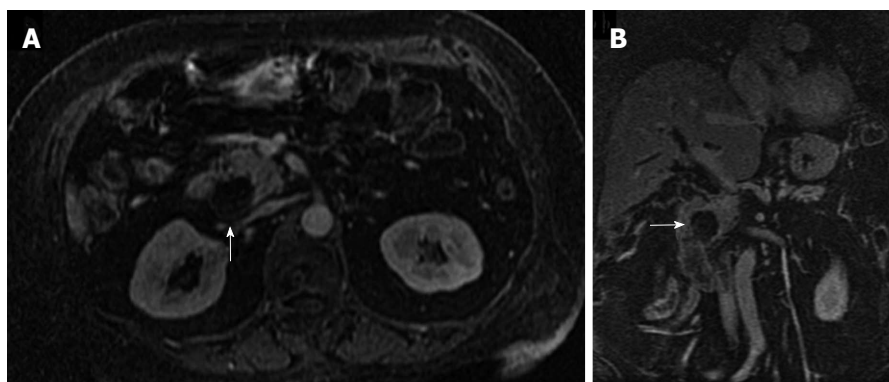

Figure 11 Axial arterial-phase gadolinium-enhanced T1-weighted fat-suppressed gradient-recalled echo magnetic resonance imaging (A) and coronal reformatted (B) show no enhancement of the hypovascular tumor in the pancreatic head (arrow). Pancreatic adenocarcinoma was proven by biopsy.
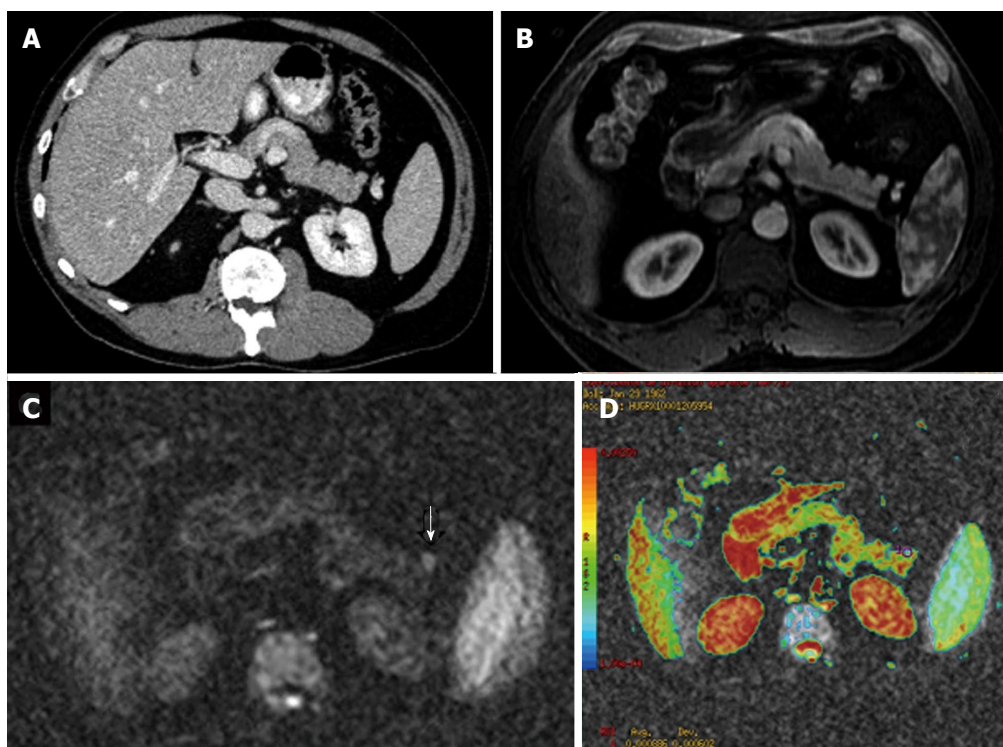

Figure 12 Use of diffusion-weighted magnetic resonance imaging in the earlier detection of pancreatic tumours. Axial contrast enhanced multidetector computed tomography image (A) and axial arterial-phase gadolinium-enhanced T1-weighted fat-suppressed gradient-recalled echo magnetic resonance image (B) do not depict any abnormality. Axial diffusion-weighted magnetic resonance imaging (C) demonstrates a focal increased signal intensity (arrow) and low apparent diffusion coefficient values in the color coded images (D).
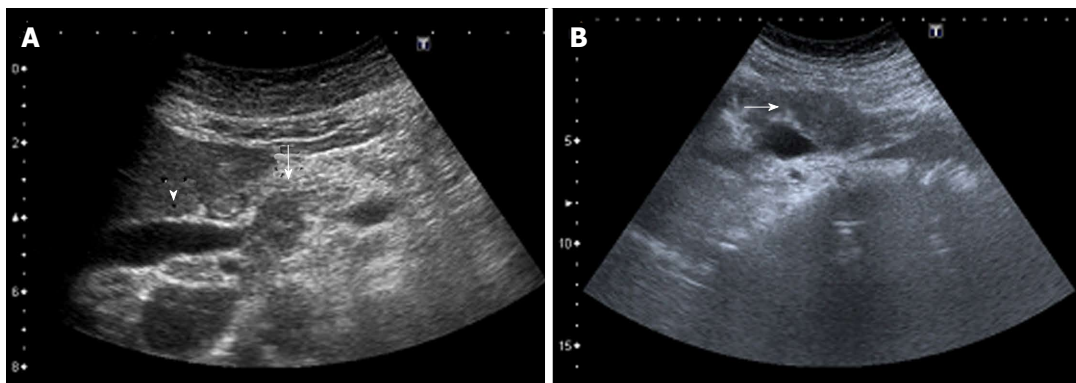
Figure 13 Ultrasound images (A, B) of an ill-defined, heterogeneous hypoechoic mass (arrow) in the pancreas obstructing the common bile duct (arrowhead).
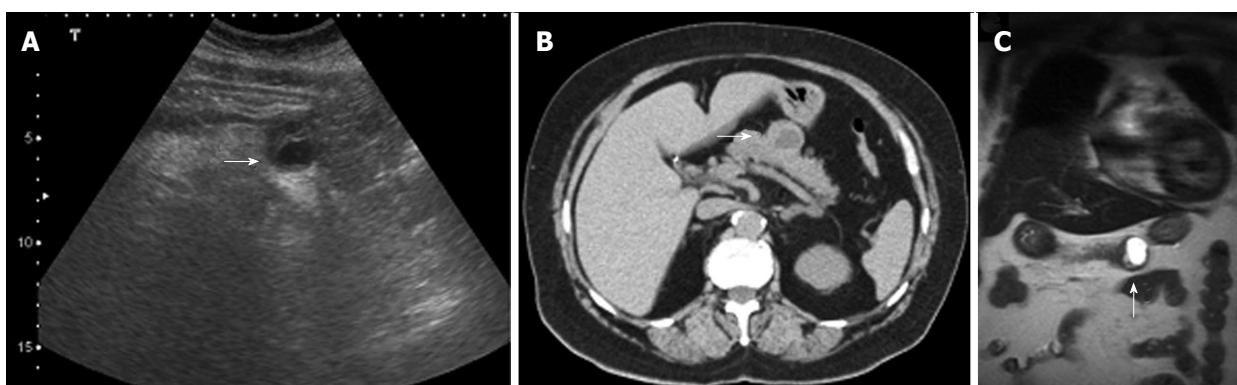

Figure 14 Pancreatic neuroendocrine tumor. Ultrasound images (A), axial unenhanced multidetector computed tomography and coronal magnetic resonance T2-weighted image show a round, heterogeneous mass, localized in the pancreatic body, with variable amounts of cystic-necrotic degeneration (arrows).
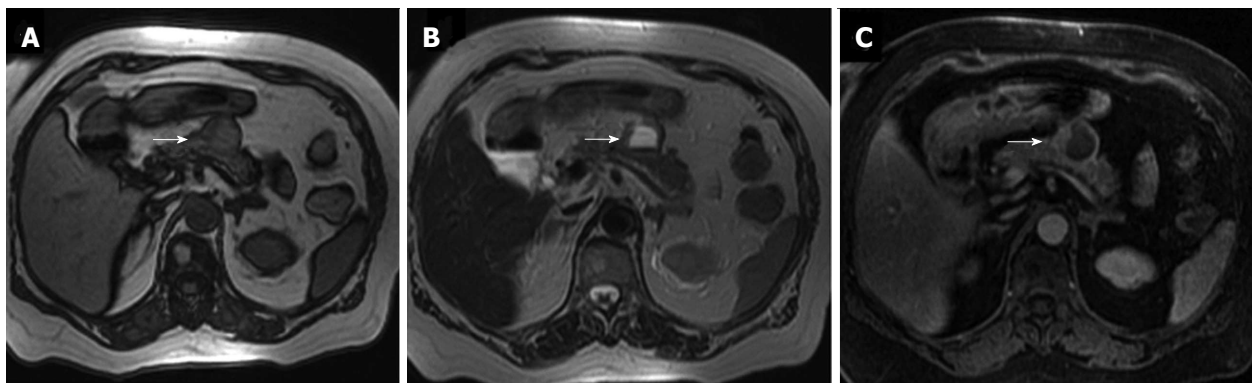

Figure 15 Same patient shown in figure 14. Magnetic resonance axial gradient T1 out-of-phase image (A) and T1 fat-suppressed sequence (C) show a hypointense signal in the liquid component of the lesion whereas it reveals a hyperintense signal in the T2-weighted sequence (B) (arrows).

organ of origin at radiology[30]. Therefore, differentiation from other pediatric tumors arising from adjacent organs (*e.g.*, neuroblastoma, Wilms tumor, hepatoblastoma) is challenging, and biopsy is generally required to establish the diagnosis. Metastases occur mostly to the liver.

At US, the mass is heterogeneous with hypoechoic cystic spaces and hyperechoic internal septa[28]. At MDCT, pancreatoblastoma generally manifests as a multiloculated inhomogeneous mass with enhancing septa[28]. On MRI the tumor has low to intermediate signal intensity on

T_1- and high signal intensity on T_2-weighted images, and shows mild contrast enhancement.

Pancreatic lymphoma
Pancreatic lymphoma is most commonly a B-cell subtype of non-Hodgkin lymphoma. Secondary lymphoma is the dominant form and is the result of direct extension from peripancreatic lymphadenopathy. Primary pancreatic lymphoma is rare, representing 0.5% of pancreatic tumors. It is more common in immunocompromised patients[31].
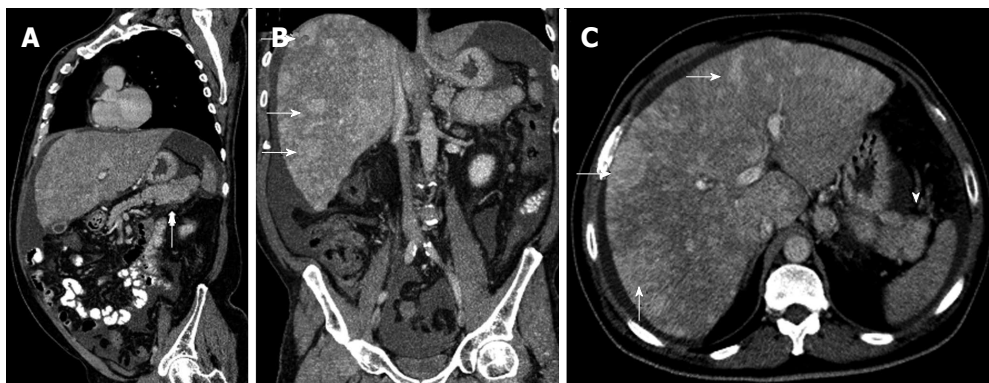
Figure 16 Sagittal multidetector computed tomography image. A: A heterogeneous pancreatic mass (arrow); B, C: Coronal (B) and axial (C) multidetector computed tomography images show multiple hypervascular metastases in the liver (arrows), showing the same enhancement pattern of the primary mass. Neuroendocrine pancreatic tumor and metastases were histologically proven.

Two morphologic patterns of pancreatic lymphoma are recognized: a focal well-circumscribed form and a diffuse form. The focal form occurs in the pancreatic head in 80% of cases and has a mean size of 8 cm. It typically has uniform low attenuation at MDCT. At MRI, it has low signal intensity on T1- and intermediate signal intensity on T2- weighted images and shows faint contrast enhancement. The diffuse form is infiltrative leading to glandular enlargement and poor definition, features that can simulate the appearance of acute pancreatitis[32,33].

CYSTIC LESIONS OF THE PANCREAS

Cystic lesions accounts for 10%-15% of all pancreatic neoplasms and represents < 5% of all malignant pancreatic tumors.

Unilocular cysts are well defined lesions without internal septa, calcification or internal soft-tissues nodules. When small (< 3 cm), these lesions are almost always benign. It is suggested to do serial imaging at 6-mo intervals for the first year and annual follow-up for a period of three years. If the cyst remains stable and the patient asymptomatic no further workup in needed[34].

Pseudocyst (encapsulated fluid collections without necrosis after 4 wk from onset of acute pancreatitis) is the most common unilocular cyst[34,35]. It is important to ask for the patient's history because a cystic lesion in a patient with a clinical history of pancreatitis is almost always a pseudocyst.

Imaging studies shows a rounded cystic mass with a thick wall. After intravenous contrast administration mild wall enhancement is demonstrated (Figure 17). If we detect a solid intracystic component, the lesion is not a pseudocyst. Other image findings that support this diagnosis are inflammation, atrophy or pancreatic calcifications. Cystic neoplasm may appear as uni or multilocular masses.

Serous cystadenoma
It is a benign lesion which typically occurs in older women. The cystic components range from millimeters to 2 cm. When the lesion grows a central scar and coarse calcification may be seen (30%). This calcified scar is highly specific and virtually pathognomonic[36] and is best demostrated at CT.

MRI shows a cluster of small cyst without visible communication within the cyst or the pancreatic duct. These cysts are hyperintense on T2-weighted images. Central calcified scar is seen as a signal void at MRI (Figure 18). Enhancement of fibrous septa between the cysts are seen on delayed images.

Mucinous cystic neoplasm (mucinous cystadenoma/ cystadenocarcinoma)
This lesion has female predominance (80%) in their sixth decade of life[37]. Mucinous cystadenoma preferentially involves the body and pancreatic tail and do not communicate with the pancreatic duct.

Cross-sectional imaging is ineffective for differentiating between mucinous cystic neoplasms with and without malignant epithelium, except in cases with invasion of adjacent organs, vascular invasion, or metastatic disease. The presence of intracystic enhancing soft tissues are suspicious for malignancy. Peripheral eggshell calcifications are not frequent (16%) but such finding is specific and has a highly predictive value for malignancy.

On US mucinous cystic neoplasms appear as hypoechogenic multilocular or, less commonly, unilocular masses with posterior acoustic enhancement. Internal septations are usually visualized and better demonstrated at US than at CT[36-40].

CT shows a round to slightly lobulated mass that is well encapsulated with smooth external margins. Because the cyst contents can vary in attenuation according to the degree of hemorrhage or protein in the mucoid cysts, different levels of attenuation may be seen within the cyst cavities[37,39,41-44] (Figure 19). After intravenous contrast administration septa and peripheral wall enhancement are detected.

At MR the lesion is hypointense on T1- and hyperintense on T2-weighted images. This lesion may be hyperintense on T1-weighted images due to mucinous content.
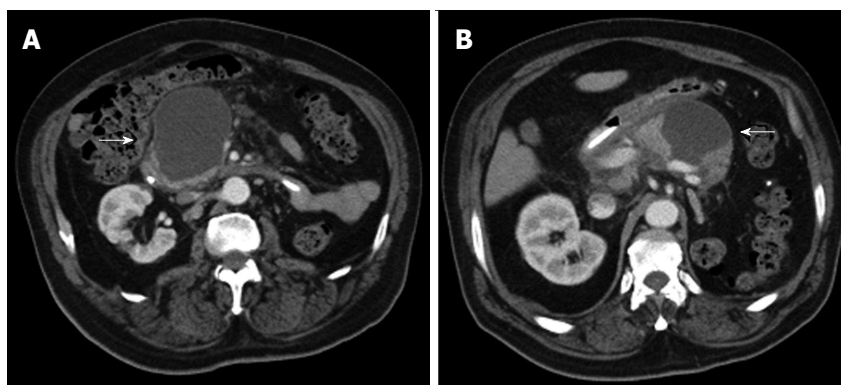
Figure 17 Axial contrast enhanced multidetector computed tomography images (A, B) reveal a homogeneously hypodense intraparenchymal fluid collection of the pancreas without any non-liquefied material in it, encapsulated completely by a thin slightly hyperdense layer (arrows). These findings are compatible with a pseudocyst in a patient with a clinical history of pancreatitis.
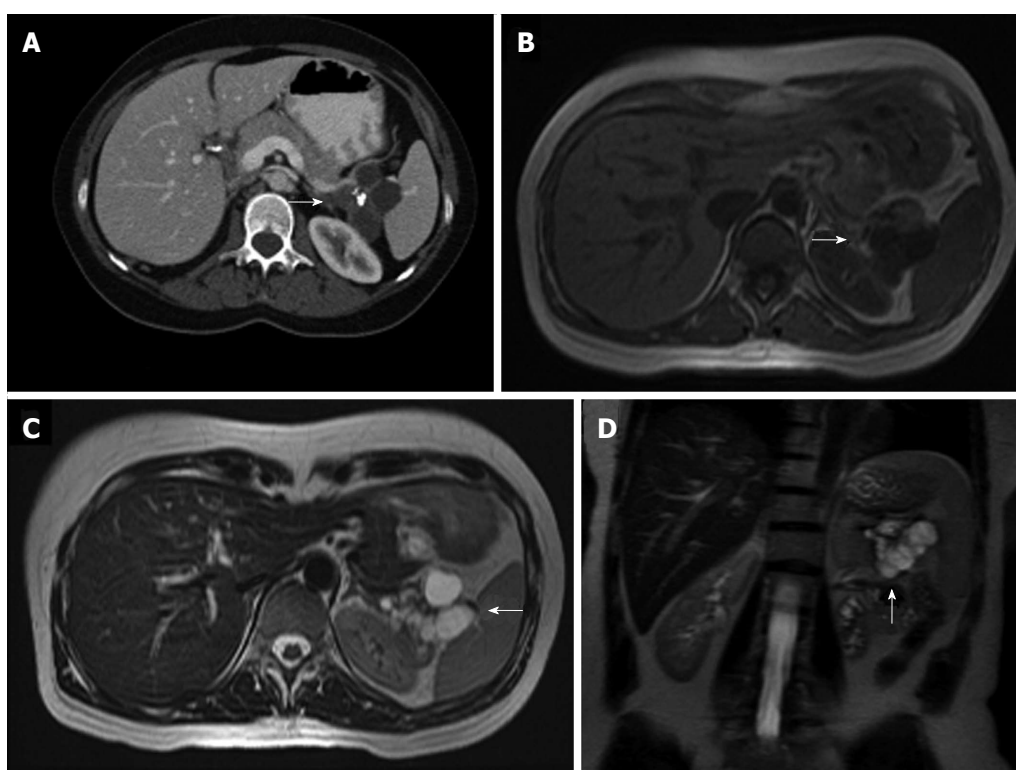

Figure 18 Axial nonenhanced multidetector computed tomography image. A: A polylobulated cystic lesion with a coarse calcification in its center (arrow), which is the phathognomonic central scar for serous cystadenoma; B-D: Magnetic resonance imaging show a cluster of small cysts (arrows), which are hypointense in T1-weighted images (B) and hyperintense in T2-weighted images (C, D), without visible communication within the cyst or the pancreatic duct. A central signal void is also identifiable.

Intraductal papillary mucinous tumor of the pancreas

Intraductal papillary mucinous tumor of the pancreas (IPMN) are most frequent indentified in elderly men. The most important features are the presence of mucin-producing tumor and cystic dilation of the main pancreatic duct, its branches or both[45,46]. The dilated ducts often contain profuse mucin. In the past, many IPMTs may have been misdiagnosed as chronic pancreatitis because of their generally benign behavior.

IPMNs may be classified as benign or malignant on the basis of the degree of dysplasia[47-50].

Preoperative determination of the presence or absence of associated invasive carcinoma is crucial; when invasive carcinoma is present, the surgical procedure may be modified to include resection of regional lymph nodes.

Main duct IPMNs are more likely to be malignant. IPMNs are frequently multifocal, and 5%-10% involve the entire pancreas.

When CT reveals a pancreatic solid mass in patients with IPMN, the lesion is probably invasive carcinoma. Other imaging features suggestive of invasive carcinoma in IPMN are the large size of the mass (> 3.5 cm), presence of mural nodules, dilatation of the main pancreatic
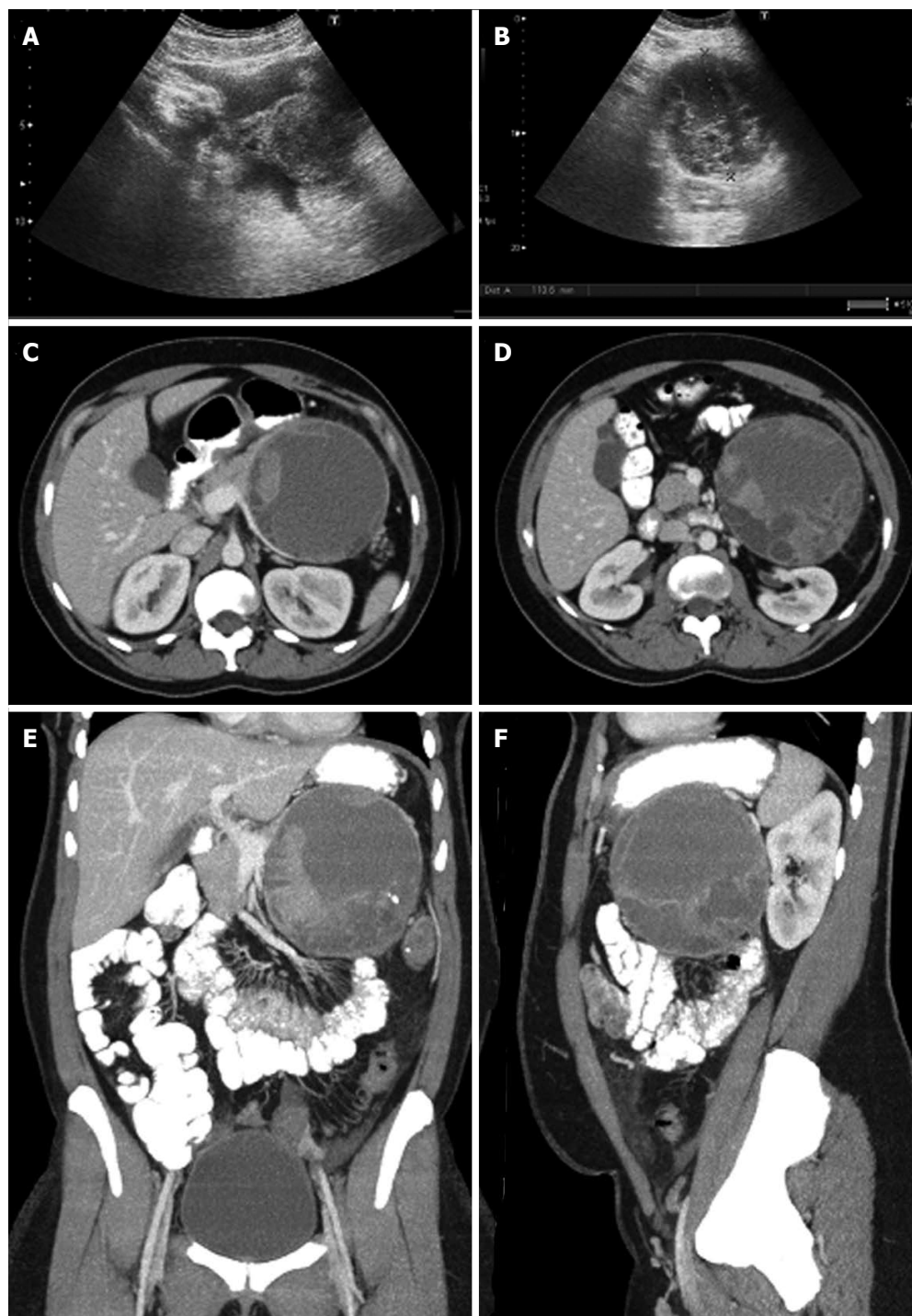
Figure 19 Ultrasound and multidetector computed tomography images. On ultrasound (A, B) a hypoechogenic multilocular mass with well-definable internal spetations and posterior acoustic enhancement can be seen. Contrast-enhanced multidetector computed tomography images (C-F) show a big round to slightly lobulated mass with an enhancing capsule and different levels of attenuation within the cyst cavities are seen. Some enhancing components are also detectable.

duct > 15 mm and multifocal involvement[49,51].

MRI is better than CT for evaluating ductal communication[52,53]. Dilatation of main pancreatic duct or multiple side branches on T2-weighted images is the most common imaging finding[54]. Demonstrating ductal communication can be useful to differentiate between IPMNs and mucinous cystadenoma (the latter has no communication with the pancreatic ductal system) (Figure 20).

Three-dimensional contrast-enhanced ultrasonography showed similar results as compared with MRI in evaluating "IPMNs" smaller than 1 cm of diameter or greater than 2 cm[55].

METASTASES TO THE PANCREAS

Pancreatic metastases account for 2%-5% of all malignant neoplasms. Metastases are most frequently from renal cell carcinoma and lung carcinoma[56]. The progno-
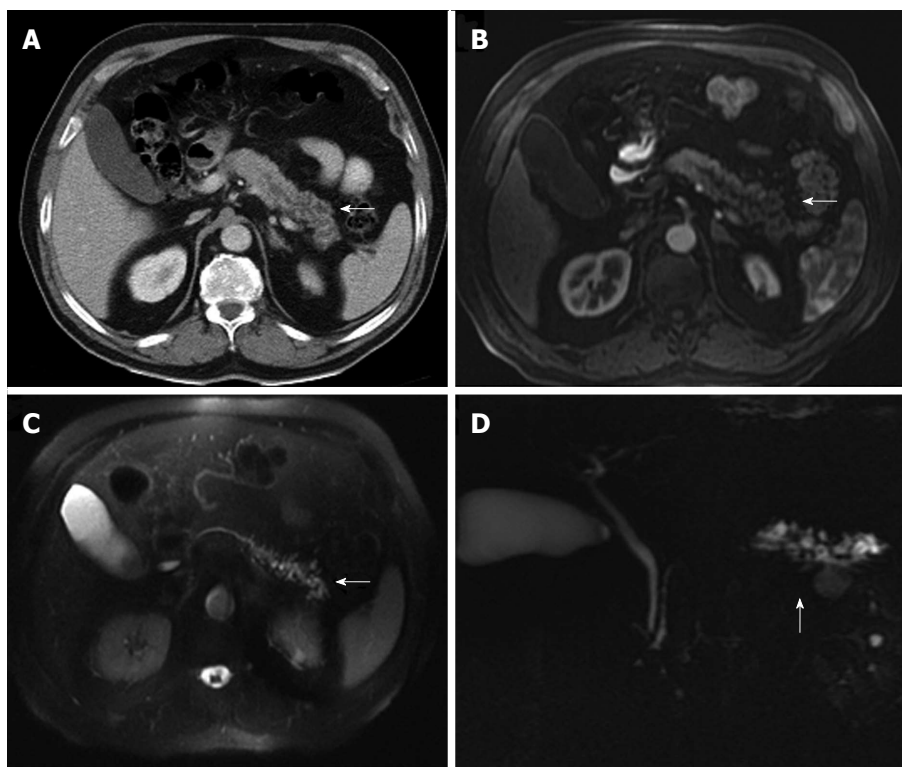
Figure 20 Multidetector computed tomography image. A: Cystic dilatation of the main pancreatic duct and some of its branches in the pancreatic tail. Ductal communication with the tumor cannot be clearly identified; B-D: In contrast-enhanced axial T1 (B) and T2-weighted (C) magnetic resonance images and in magnetic resonance imaging cholangiography (D) ductal communication can be easily detectable.

sis is generally more favorable than that for pancreatic adenocarcinoma[3] (Figure 21).

Three morphologic patterns of involvement are recognized: solitary (50%-70%), multifocal and diffuse[56,57]. At contrast-enhanced CT and MR imaging, the appearances of pancreatic metastases closely resemble that of primary carcinoma but pancreatic adenocarcinoma generally manifests as a hypoenhancing mass, whereas metastases show either peripheral enhancement (in lesions > 1.5 cm) or, less commonly, homogeneous enhancement (smaller lesions)[56,58,59].

Cystic metastases to the pancreas cannot be differentiated from mucinous cystic neoplasms radiographically. Ovarian carcinoma metastases are the most likely to manifest as a predominantly cystic mass.

A known history of primary malignant disease, combined with the presence of other metastatic foci, are helpful clues in making the diagnosis.

INTRAOPERATIVE ULTRA-SONOGRAPHY OF THE PANCREAS

Up to 40% of patients with pancreatic adenocarcinoma judged resectable at CT are found to have unresectable lesions at surgery[60,61]. Laparoscopy intraoperative US may be useful before open surgical resection to decrease the number of patients who undergo needless open surgery for resection of a tumor that ultimately proves unresectable[62]. Pancreatic adenocarcinoma appears at intraoperative US as a hypoechoic mass with ill-defined

margins[60].

EVALUATION OF THE POSTOPERATIVE PANCREAS

The most common complications of the Whipple procedure are delayed gastric emptying, pancreatic fistulas, wound infection, abdominal abscess, intraabdominal bleeding, and anastomotic leakage. A pancreaticojejunal fistula is diagnosed clinically on the basis of the detection of amylase-rich fluid in the drainage. Anastomotic leaks usually occur at the pancreaticojejunal anastomosis during first 2 wk after pancreatoduodenectomy and these leaks can be diagnosed on the basis of the presence of oral contrast material in the peritoneal cavity and are associated with peripancreatic fluid collections[63,64].

Locally recurrent disease is sometimes difficult to depict on the earliest postoperative images. Locally recurrent disease appears as an infiltrating mass with soft-tissue attenuation, perineural invasion and encasement of the mesenteric vessels[65]. Perivascular cuffing in the mesenteric fat is likely inflammatory in patients with negative surgical margins and should not be mistaken for local recurrence[63].

CONCLUSION

The knowledge of some of the most important characteristic key findings of pancreatic tumors may facilitate radiologists, and especially radiographers in training,
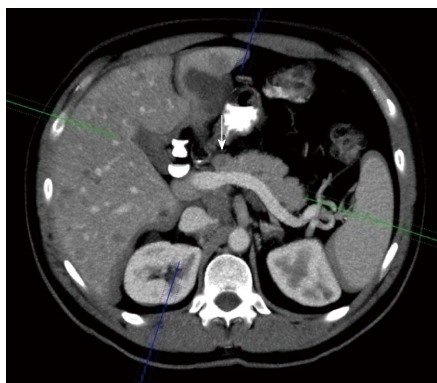
Figure 21 Oblique reformatted enhanced multidetector computed tomography image reveals a well-defined round mass in the pancreas, slightly hypodense to the pancreatic parenchyma. Pancreatic metastases from melanoma was proven. Note the liver concomitant metastases.

to do an accurate detection and staging of pancreatic neoplams in order to ensure an appropriate selection of patients who will benefit from surgery and prevent unnecessary surgeries in patients with unresectable disease.

REFERENCES

1   **Lu DS**, Reber HA, Krasny RM, Kadell BM, Sayre J. Local staging of pancreatic cancer: criteria for unresectability of major vessels as revealed by pancreatic-phase, thin-section helical CT. *AJR Am J Roentgenol* 1997; **168**: 1439-1443 [PMID: 9168704 DOI: 10.2214/ajr.168.6.9168704]

2   **Brennan DD**, Zamboni GA, Raptopoulos VD, Kruskal JB. Comprehensive preoperative assessment of pancreatic adenocarcinoma with 64-section volumetric CT. *Radiographics* 2007; **27**: 1653-1666 [PMID: 18025509 DOI: 10.1148/rg.276075034]

3   **Low G**, Panu A, Millo N, Leen E. Multimodality imaging of neoplastic and nonneoplastic solid lesions of the pancreas. *Radiographics* 2011; **31**: 993-1015 [PMID: 21768235 DOI: 10.1148/rg.314105731]

4   **Ros PR**, Mortelé KJ. Imaging features of pancreatic neoplasms. *JBR-BTR* 2001; **84**: 239-249 [PMID: 11817475]

5   **Ross BA**, Jeffrey RB, Mindelzun RE. Normal variations in the lateral contour of the head and neck of the pancreas mimicking neoplasm: evaluation with dual-phase helical CT. *AJR Am J Roentgenol* 1996; **166**: 799-801 [PMID: 8610553 DOI: 10.2214/ajr.166.4.8610553]

6   **Lawler LP**, Horton KM, Fishman EK. Peripancreatic masses that simulate pancreatic disease: spectrum of disease and role of CT. *Radiographics* 2003; **23**: 1117-1131 [PMID: 12975504 DOI: 10.1148/rg.235035013]

7   **Grand DJ**, Sobin LH, Fishman EK. Enteric duplication cyst of the pancreas: CT findings. *Crit Rev Comput Tomogr* 2004; **45**: 105-110 [PMID: 15222235 DOI: 10.3109/1040837049040023]

8   **Bidet AC**, Dreyfus-Schmidt G, Mas J, Combe J, Milleret P, Bidet R. Diagnosis of splenosis: the advantages of splenic scintiscanning with Tc 99m heat-damaged red blood cells. *Eur J Nucl Med* 1986; **12**: 357-358 [PMID: 3792367 DOI: 10.1007/BF00263820]

9   **Johnson PT**, Outwater EK. Pancreatic carcinoma versus chronic pancreatitis: dynamic MR imaging. *Radiology* 1999; **212**: 213-218 [PMID: 10405744]

10 **Nagamachi S**, Nishii R, Wakamatsu H, Mizutani Y, Kiyohara S, Fujita S, Futami S, Sakae T, Furukoji E, Tamura S, Arita H, Chijiiwa K, Kawai K. The usefulness of (18)F-FDG PET/MRI fusion image in diagnosing pancreatic tumor: comparison with (18)F-FDG PET/CT. *Ann Nucl Med* 2013; **27**: 554-563

11 **Phatak MG**, Hill BJ, Bonus RL, Baker D, Sharif MM. Dilated extrahepatic ducts simulating low density mass in the region of the head of the pancreas-a case report. *Comput Radiol* 1982; **6**: 115-118 [PMID: 7083840 DOI: 10.1016/0730-4862(82)90154-8]

12 **Hough TJ**, Raptopoulos V, Siewert B, Matthews JB. Teardrop superior mesenteric vein: CT sign for unresectable carcinoma of the pancreas. *AJR Am J Roentgenol* 1999; **173**: 1509-1512 [PMID: 10584793 DOI: 10.2214/ajr.173.6310584793]

13 **Kosmahl M**, Pauser U, Anlauf M, Klöppel G. Pancreatic ductal adenocarcinomas with cystic features: neither rare nor uniform. *Mod Pathol* 2005; **18**: 1157-1164 [PMID: 15920540 DOI: 10.1038/modpathol.3800446]

14 **Kim SY**, Park SH, Hong N, Kim JH, Hong SM. Primary solid pancreatic tumors: recent imaging findings updates with pathology correlation. *Abdom Imaging* 2013; **38**: 1091-1105 [PMID: 23640523]

15 **Hanbidge AE**. Cancer of the pancreas: the best image for early detection--CT, MRI, PET or US? *Can J Gastroenterol* 2002; **16**: 101-105 [PMID: 11875594]

16 **Wang Y**, Miller FH, Chen ZE, Merrick L, Mortele KJ, Hoff FL, Hammond NA, Yaghmai V, Nikolaidis P. Diffusion-weighted MR imaging of solid and cystic lesions of the pancreas. *Radiographics* 2011; **31**: E47-E64 [PMID: 21721197 DOI: 10.1148/rg.313105174]

17 **Kartalis N**, Lindholm TL, Aspelin P, Permert J, Albiin N. Diffusion-weighted magnetic resonance imaging of pancreas tumours. *Eur Radiol* 2009; **19**: 1981-1990 [PMID: 19308414 DOI: 10.1007/s00330-009-1384-8]

18 **Le Bihan D**, Breton E, Lallemand D, Aubin ML, Vignaud J, Laval-Jeantet M. Separation of diffusion and perfusion in intravoxel incoherent motion MR imaging. *Radiology* 1988; **168**: 497-505 [PMID: 3393671]

19 **Noone TC**, Hosey J, Firat Z, Semelka RC. Imaging and localization of islet-cell tumours of the pancreas on CT and MRI. *Best Pract Res Clin Endocrinol Metab* 2005; **19**: 195-211 [PMID: 15763695 DOI: 10.1016/j.beem.2004.11.013]

20 **Wallace D**. Endocrine Tumors of the Pancreas. Practical Gastroenterology, 2012

21 **Buetow PC**, Buck JL, Pantongrag-Brown L, Beck KG, Ros PR, Adair CF. Solid and papillary epithelial neoplasm of the pancreas: imaging-pathologic correlation on 56 cases. *Radiology* 1996; **199**: 707-711 [PMID: 8637992]

22 **Yao X**, Ji Y, Zeng M, Rao S, Yang B. Solid pseudopapillary tumor of the pancreas: cross-sectional imaging and pathologic correlation. *Pancreas* 2010; **39**: 486-491 [PMID: 19940797 DOI: 10.1097/MPA.0b013e3181bd6839]

23 **Dong PR**, Lu DS, Degregario F, Fell SC, Au A, Kadell BM. Solid and papillary neoplasm of the pancreas: radiological-pathological study of five cases and review of the literature. *Clin Radiol* 1996; **51**: 702-705 [PMID: 8893639 DOI: 10.1016/S0009-9260(96)80242-X]

24 **Cantisani V**, Mortele KJ, Levy A, Glickman JN, Ricci P, Passariello R, Ros PR, Silverman SG. MR imaging features of solid pseudopapillary tumor of the pancreas in adult and pediatric patients. *AJR Am J Roentgenol* 2003; **181**: 395-401 [PMID: 12876017 DOI: 10.2214/ajr.181.2.1810395]

25 **Kehagias D**, Smyrniotis V, Gouliamos A, Vlahos L. Cystic pancreatic neoplasms: computed tomography and magnetic resonance imaging findings. *Int J Pancreatol* 2000; **28**: 223-230 [PMID: 11373061]

26 **Coleman KM**, Doherty MC, Bigler SA. Solid-pseudopapillary tumor of the pancreas. *Radiographics* 2003; **23**: 1644-1648 [PMID: 14615569 DOI: 10.1148/rg.236035008]

27 **Al-Qahtani S**, Gudinchet F, Laswed T, Schnyder P, Schmidt S, Osterheld MC, Alamo L. Solid pseudopapillary tumor of the pancreas in children: typical radiological findings and pathological correlation. *Clin Imaging* 2010; **34**: 152-156 [PMID: 20189082 DOI: 10.1016/j.clinimag.2009.06.024]

28 **Chung EM**, Travis MD, Conran RM. Pancreatic tumors in children: radiologic-pathologic correlation. *Radiograph-*

ics 2006; **26**: 1211-1238 [PMID: 16844942 DOI: 10.1148/rg.264065012]

29 **Winter JM**, Cameron JL, Lillemoe KD, Campbell KA, Chang D, Riall TS, Coleman J, Sauter PK, Canto M, Hruban RH, Schulick RD, Choti MA, Yeo CJ. Periampullary and pancreatic incidentaloma: a single institution's experience with an increasingly common diagnosis. *Ann Surg* 2006; **243**: 673-680; discussion 680-683 [PMID: 16633003 DOI: 10.1097/01.sla.0000216763.27673.97]

30 **Montemarano H**, Lonergan GJ, Bulas DI, Selby DM. Pancreatoblastoma: imaging findings in 10 patients and review of the literature. *Radiology* 2000; **214**: 476-482 [PMID: 10671596]

31 **Zucca E**, Roggero E, Bertoni F, Cavalli F. Primary extranodal non-Hodgkin's lymphomas. Part 1: Gastrointestinal, cutaneous and genitourinary lymphomas. *Ann Oncol* 1997; **8**: 727-737 [PMID: 9332679 DOI: 10.1023/A]

32 **Nayer H**, Weir EG, Sheth S, Ali SZ. Primary pancreatic lymphomas: a cytopathologic analysis of a rare malignancy. *Cancer* 2004; **102**: 315-321 [PMID: 15386314 DOI: 10.1002/cncr.20488]

33 **Merkle EM**, Bender GN, Brambs HJ. Imaging findings in pancreatic lymphoma: differential aspects. *AJR Am J Roentgenol* 2000; **174**: 671-675 [PMID: 10701607 DOI: 10.2214/ajr.174.3.1740671]

34 **Allen PJ**, Jaques DP, D'Angelica M, Bowne WB, Conlon KC, Brennan MF. Cystic lesions of the pancreas: selection criteria for operative and nonoperative management in 209 patients. *J Gastrointest Surg* 2003; **7**: 970-977 [PMID: 14675706 DOI: 10.1016/j.gassur.2003.08.008]

35 **Thoeni RF**. The revised Atlanta classification of acute pancreatitis: its importance for the radiologist and its effect on treatment. *Radiology* 2012; **262**: 751-764 [PMID: 22357880 DOI: 10.1148/radiol.11110947]

36 **Sahani DV**, Kadavigere R, Saokar A, Fernandez-del Castillo C, Brugge WR, Hahn PF. Cystic pancreatic lesions: a simple imaging-based classification system for guiding management. *Radiographics* 2005; **25**: 1471-1484 [PMID: 16284129 DOI: 10,1148/rg.256045161]

37 **Friedman AC**, Lichtenstein JE, Dachman AH. Cystic neoplasms of the pancreas. Radiological-pathological correlation. *Radiology* 1983; **149**: 45-50 [PMID: 6611949]

38 **Johnson CD**, Stephens DH, Charboneau JW, Carpenter HA, Welch TJ. Cystic pancreatic tumors: CT and sonographic assessment. *AJR Am J Roentgenol* 1988; **151**: 1133-1138 [PMID: 3055888 DOI: 10.2214/ajr.151.61133]

39 **Fugazzola C**, Procacci C, Bergamo Andreis IA, Iacono C, Portuese A, Dompieri P, Laveneziana S, Zampieri PG, Jannucci A, Serio G. Cystic tumors of the pancreas: evaluation by ultrasonography and computed tomography. *Gastrointest Radiol* 1991; **16**: 53-61 [PMID: 1991611 DOI: 10.1007/BF01887305]

40 **Rumack CM**, Wilson SR, Charboneau JW. Diagnostic Ultrasound. Amsterdam: Elsevier Mosby, 2011

41 **Minami M**, Itai Y, Ohtomo K, Yoshida H, Yoshikawa K, Iio M. Cystic neoplasms of the pancreas: comparison of MR imaging with CT. *Radiology* 1989; **171**: 53-56 [PMID: 2928546]

42 **Soyer P**, Rabenandrasana A, Van Beers B, Barge J, Sibert A, Laissy JP, Achour E, Levesque M. Cystic tumors of the pancreas: dynamic CT studies. *J Comput Assist Tomogr* 1994; **18**: 420-426 [PMID: 8188910 DOI: 10.1097/00004728-199405000-00015]

43 **Ichikawa T**, Sou H, Araki T, Arbab AS, Yoshikawa T, Ishigame K, Haradome H, Hachiya J. Duct-penetrating sign at MRCP: usefulness for differentiating inflammatory pancreatic mass from pancreatic carcinomas. *Radiology* 2001; **221**: 107-116 [PMID: 11568327 DOI: 10.1148/radiol.2211001157]

44 **Parienty RA**, Ducellier R, Lubrano JM, Picard JD, Pradel J, Smolarski N. Cystadenomas of the pancreas: diagnosis by computed tomography. *J Comput Assist Tomogr* 1980; **4**: 364-367 [PMID: 7372868 DOI: 10.1097/00004728-198006000-0001]

45 **Lim JH**, Lee G, Oh YL. Radiologic spectrum of intraductal papillary mucinous tumor of the pancreas. *Radiographics* 2001; **21**: 323-337; discussion 337-340 [PMID: 11259696]

46 **Procacci C**, Graziani R, Bicego E, Bergamo-Andreis IA, Mainardi P, Zamboni G, Pederzoli P, Cavallini G, Valdo M, Pistolesi GF. Intraductal mucin-producing tumors of the pancreas: imaging findings. *Radiology* 1996; **198**: 249-257 [PMID: 8539388]

47 **Longnecker DS**, Adler G, Hruban RH. Intraductal papillary-mucinous neoplasms of the pancreas. *J Pancreas* 2000; **11**: 249–254

48 **Ban S**, Naitoh Y, Mino-Kenudson M, Sakurai T, Kuroda M, Koyama I, Lauwers GY, Shimizu M. Intraductal papillary mucinous neoplasm (IPMN) of the pancreas: its histopathologic difference between 2 major types. *Am J Surg Pathol* 2006; **30**: 1561-1569 [PMID: 17122512 DOI: 10.1097/01.pas.0000213305.98187.d4]

49 **Vullierme MP**, Giraud-Cohen M, Hammel P, Sauvanet A, Couvelard A, O'Toole D, Levy P, Ruszniewski P, Vilgrain V. Malignant intraductal papillary mucinous neoplasm of the pancreas: in situ versus invasive carcinoma surgical resectability. *Radiology* 2007; **245**: 483-490 [PMID: 17848678 DOI: 10.1148/radiol.2451060951]

50 **Hruban RH**, Takaori K, Klimstra DS, Adsay NV, Albores-Saavedra J, Biankin AV, Biankin SA, Compton C, Fukushima N, Furukawa T, Goggins M, Kato Y, Klöppel G, Longnecker DS, Lüttges J, Maitra A, Offerhaus GJ, Shimizu M, Yonezawa S. An illustrated consensus on the classification of pancreatic intraepithelial neoplasia and intraductal papillary mucinous neoplasms. *Am J Surg Pathol* 2004; **28**: 977-987 [PMID: 15252303 DOI: 10.1097/01.pas.0000126675.59108.80]

51 **Kawamoto S**, Horton KM, Lawler LP, Hruban RH, Fishman EK. Intraductal papillary mucinous neoplasm of the pancreas: can benign lesions be differentiated from malignant lesions with multidetector CT? *Radiographics* 2005; **25**: 1451-1468; discussion 1468-1470 [PMID: 16284127 DOI: 10.1148/rg.256055036]

52 **Song SJ**, Lee JM, Kim YJ, Kim SH, Lee JY, Han JK, Choi BI. Differentiation of intraductal papillary mucinous neoplasms from other pancreatic cystic masses: comparison of multirow-detector CT and MR imaging using ROC analysis. *J Magn Reson Imaging* 2007; **26**: 86-93 [PMID: 17659551 DOI: 10.1002/jmri.21001]

53 **Waters JA**, Schmidt CM, Pinchot JW, White PB, Cummings OW, Pitt HA, Sandrasegaran K, Akisik F, Howard TJ, Nakeeb A, Zyromski NJ, Lillemoe KD. CT vs MRCP: optimal classification of IPMN type and extent. *J Gastrointest Surg* 2008; **12**: 101-109 [PMID: 17917784 DOI: 10.1007/s11605-007-0367-9]

54 **Procacci C**, Megibow AJ, Carbognin G, Guarise A, Spoto E, Biasiutti C, Pistolesi GF. Intraductal papillary mucinous tumor of the pancreas: a pictorial essay. *Radiographics* 1999; **19**: 1447-1463 [PMID: 10555668]

55 **Pezzilli R**, Serra C, Calculli L, Ferroni F, Iammarino MT, Casadei R. Three-dimensional contrast-enhanced ultrasonography of intraductal papillary mucinous neoplasms of the pancreas: a comparison with magnetic resonance imaging. *Pancreas* 2013; **42**: 1164-1168 [PMID: 23770711]

56 **Tsitouridis I**, Diamantopoulou A, Michaelides M, Arvanity M, Papaioannou S. Pancreatic metastases: CT and MRI findings. *Diagn Interv Radiol* 2010; **16**: 45-51 [PMID: 20027546]

57 **Muranaka T**, Teshima K, Honda H, Nanjo T, Hanada K, Oshiumi Y. Computed tomography and histologic appearance of pancreatic metastases from distant sources. *Acta Radiol* 1989; **30**: 615-619 [PMID: 2631949 DOI: 10.3109/02841858909174725]

58 **Kelekis NL**, Semelka RC, Siegelman ES. MRI of pancreatic metastases from renal cancer. *J Comput Assist Tomogr* 1996; **20**: 249-253 [PMID: 8606232]

59 **Klein KA**, Stephens DH, Welch TJ. CT characteristics of metastatic disease of the pancreas. *Radiographics* 1998; **18**:

369-378 [PMID: 9536484]

60 **Sun MR**, Brennan DD, Kruskal JB, Kane RA. Intraoperative ultrasonography of the pancreas. *Radiographics* 2010; **30**: 1935-1953 [PMID: 21057128 DOI: 10.1148/rg.307105051]

61 **D'Onofrio M**, Barbi E, Robertis R, Principe F, Gallotti A, Martone E. Intraoperative Ultrasonography of the Pancreas. Milano: Ultrasonography of the Pancreas, 2012: 55–61

62 **Doucas H**, Sutton CD, Zimmerman A, Dennison AR, Berry DP. Assessment of pancreatic malignancy with laparoscopy and intraoperative ultrasound. *Surg Endosc* 2007; **21**: 1147-1152 [PMID: 17177081 DOI: 10.1007/s00464-006-9093-8]

63 **Yamauchi FI**, Ortega CD, Blasbalg R, Rocha MS, Jukemura J,

Cerri GG. Multidetector CT evaluation of the postoperative pancreas. *Radiographics* 2012; **32**: 743-764 [PMID: 22582357 DOI: 10.1148/rg.323105121]

64 **Riediger H**, Makowiec F, Schareck WD, Hopt UT, Adam U. Delayed gastric emptying after pylorus-preserving pancreatoduodenectomy is strongly related to other postoperative complications. *J Gastrointest Surg* 2003; **7**: 758-765 [PMID: 13129553 DOI: 10.1016/S1091-255X(03)00109-4]

65 **Bluemke DA**, Abrams RA, Yeo CJ, Cameron JL, Fishman EK. Recurrent pancreatic adenocarcinoma: spiral CT evaluation following the Whipple procedure. *Radiographics* 1997; **17**: 303-313 [PMID: 9084073]